

Double-lepton polarization asymmetries in $\Lambda_b \rightarrow \Lambda \ell^+ \ell^-$ decay in universal extra dimension model

T.M. Aliev^{1,a}, M. Savcı^{1,b}, B.B. Şirvanlı^{2,c}

¹ Physics Department, Middle East Technical University, İnönü Bulvarı, 06531 Ankara, Turkey

² Physics Department, Gazi University, 06500 Teknik Okullar, Ankara, Turkey

Received: 7 October 2006 / Revised version: 24 May 2007 /

Published online: 10 August 2007 – © Springer-Verlag / Società Italiana di Fisica 2007

Abstract. Double-lepton polarization asymmetries in $\Lambda_b \rightarrow \Lambda \ell^+ \ell^-$ decay are calculated in the universal extra dimension (UED) model. It is found that numerous double-lepton polarization asymmetries are very sensitive to the UED model and therefore can be a very useful tool for establishing new physics predicted by the UED model.

PACS. 12.60.-i; 13.30.-a; 14.20.Mr

1 Introduction

Despite the impressive success of the standard model (SM) in describing all existing experimental data, it is commonly believed that SM is the low energy limit of a more fundamental theory. There are two different ways of looking for evidence for new physics beyond the SM:

- direct production of new particles at high energy colliders like LHC;
- signals of new interactions and particles can be obtained indirectly through the analysis of rare decays.

Rare B meson decays induced by the $b \rightarrow s(d)$ transitions play a special role, since they are forbidden at tree level in the SM and appear only at quantum (one-loop) level. Moreover, these decays are the most promising ones for establishing new physics. New physics in these decays can appear either through the differences in the Wilson coefficients from the ones existing in the SM or through new operator structures in the effective Hamiltonian, which are absent in the SM.

Among all decay channels of B mesons, semileptonic ones receive special interest. These decays are theoretically more or less clean, and they have a relatively large branching ratio. These decays contain many physically measurable quantities, like the forward–backward asymmetry \mathcal{A}_{FB} , lepton polarization asymmetries, etc., which are very useful and serve as a testing ground for the SM and are useful for looking for new physics beyond the SM [1]. From the experimental side, the BELLE [2, 3] and

BaBar [4, 5] collaborations provide recent measurements of the branching ratios of the semileptonic decays due to the $b \rightarrow s \ell^+ \ell^-$ transitions, which can be summarized as follows:

$$\mathcal{B}(B \rightarrow K^* \ell^+ \ell^-) = \begin{cases} (16.5_{-2.2}^{+2.3} \pm 0.9 \pm 0.4) \times 10^{-7} [2], \\ (7.8_{-1.7}^{+1.9} \pm 1.2) \times 10^{-7} [4], \end{cases}$$

$$\mathcal{B}(B \rightarrow K \ell^+ \ell^-) = \begin{cases} (5.5_{-0.70}^{+0.75} \pm 0.27 \pm 0.02) \times 10^{-7} [2], \\ (3.4 \pm 0.7 \pm 0.3) \times 10^{-7} [4], \end{cases}$$

$$\mathcal{B}(B \rightarrow X_s \ell^+ \ell^-) = \begin{cases} (4.11 \pm 0.83_{-0.81}^{+0.85}) \times 10^{-6} [3], \\ (5.6 \pm 1.5 \pm 0.6 \pm 1.1) \times 10^{-6} [5]. \end{cases}$$

Another exclusive decay that is described at the inclusive level by the $b \rightarrow s \ell^+ \ell^-$ transition is baryonic $\Lambda_b \rightarrow \Lambda \ell^+ \ell^-$ decay. Unlike mesonic decays, the baryonic decays could maintain the helicity structure of the effective Hamiltonian for the $b \rightarrow s$ transition [6]. Radiative and semileptonic decays of Λ_b such as $\Lambda_b \rightarrow \Lambda \gamma$, $\Lambda_b \rightarrow \Lambda_c \ell \bar{\nu}_\ell$, $\Lambda_b \rightarrow \Lambda \ell^+ \ell^-$ ($\ell = e, \mu, \tau$) and $\Lambda_b \rightarrow \Lambda \nu \bar{\nu}$ have been studied extensively in the literature [7–21] (see also [1] and references therein). More about heavy baryons, including the experimental prospects, can be found in [22, 23].

It is noted in [24] that some of the single-lepton polarization asymmetries might be too small to be observed and therefore might not provide a sufficient number of observables for checking the structure of the effective Hamiltonian. In order to obtain more observables, London et al. proposed to take polarizations of both leptons into account [24], which are simultaneously measurable. Along

^a e-mail: taliev@metu.edu.tr

permanent address: Institute of Physics, Baku, Azerbaijan

^b e-mail: savci@verdi.physics.metu.edu.tr

^c e-mail: bbelma@gazi.edu.tr

these lines the maximum number of independent polarization observables are constructed in [24].

Among the various models of physics beyond the SM, extra dimensions attract special interest, because they include gravity in addition to other interactions, giving hints on the hierarchy problem and a connection with string theory. The model of Appelquist, Cheng and Dobrescu (ACD) [25] with one universal extra dimension (UED), where all the SM particles can propagate in the extra dimension, is very attractive (see also [26]). Compactification of the extra dimension leads to the Kaluza–Klein model in the four-dimensional case. In this model, the only additional free parameter with respect to the SM is $1/R$, i.e., the inverse of the compactification radius.

The restrictions imposed on UED are examined in the current accelerators; for example, Tevatron experiments put the bound at about $1/R \geq 300$ GeV. Analysis of the anomalous magnetic moment [27, 28] and the $Z \rightarrow \bar{b}b$ vertex [29] also lead to the bound $1/R \geq 300$ GeV.

A possible manifestation of UED models in the K_L – K_S mass difference, the parameter ε_K , B – \bar{B}_0 mixing, the mass difference $\Delta M_{d,s}$, and the rare decays $K^+ \rightarrow \pi \bar{\nu} \nu$, $K_L \rightarrow \pi^0 \bar{\nu} \nu$, $K_L \rightarrow \mu^+ \mu^-$, $B \rightarrow X_{s,d} \bar{\nu} \nu$, $B_{s,d} \rightarrow \mu^+ \mu^-$, $B \rightarrow X_s \gamma$, $B \rightarrow X_s \text{gluon}$, $B \rightarrow X_s \mu^+ \mu^-$ and ε'/ε are comprehensively investigated in [30, 31]. Exclusive $B \rightarrow K^* \ell^+ \ell^-$, $B \rightarrow K^* \bar{\nu} \nu$ and $B \rightarrow K^* \gamma$ decays are studied in the framework of the UED scenario in [32], and $\Lambda_b \rightarrow \Lambda \ell^+ \ell^-$ is treated in the UED model in [33]. It is shown in [32] that the most stringent bound on R comes from the $B \rightarrow K^* \gamma$ decay, restricting R to the values $1/R \geq 250$ GeV, which we will use in our numerical calculations.

In the present work we study the double-lepton polarization asymmetries for $\Lambda_b \rightarrow \Lambda \ell^+ \ell^-$ decay in the UED model. The plan of the paper is as follows. In Sect. 2 we briefly discuss the main ingredients of ACD model and calculate all possible double-lepton polarization asymmetries for the rare $\Lambda_b \rightarrow \Lambda \ell^+ \ell^-$ decay. Section 3 is devoted to a numerical analysis and conclusions.

2 $\Lambda_b \rightarrow \Lambda \ell^+ \ell^-$ decay in ACD model

Let us remind the interested reader of the main ingredients of the simplest ACD model, which is the minimal extension of the SM in $4+1$ dimensions. The five-dimensional ACD model with a single UED uses orbifold compactification; namely, the fifth dimension y that is compactified in a circle of radius R , with the points $y=0$ and $y=\pi R$ fixed points of the orbifolds. Generalization of the SM is realized by the propagating fermions, gauge bosons and the Higgs fields in all five dimensions. The Lagrangian in ACD can be written as

$$\mathcal{L} = \int d^4x dy \{ \mathcal{L}_A + \mathcal{L}_H + \mathcal{L}_F + \mathcal{L}_Y \},$$

where

$$\begin{aligned} \mathcal{L}_A &= -\frac{1}{4} W^{MNa} W_{MN}^a - \frac{1}{4} B^{MN} B_{MN}, \\ \mathcal{L}_H &= (\mathcal{D}^M \phi)^\dagger \mathcal{D}_M \phi - V(\phi), \end{aligned}$$

$$\begin{aligned} \mathcal{L}_F &= \bar{Q} (i\Gamma^M \mathcal{D}_M) Q + \bar{U} (i\Gamma^M \mathcal{D}_M) U + \bar{D} (i\Gamma^M \mathcal{D}_M) D, \\ \mathcal{L}_Y &= -\bar{Q} \tilde{Y}_u \phi^c U - \bar{Q} \tilde{Y}_d \phi D + \text{h.c.} \end{aligned}$$

Here M and N running over $0, 1, 2, 3, 5$ are the five-dimensional Lorentz indices, $W_{MN}^a = \partial_M W_N^a - \partial_N W_M^a + \tilde{g} \varepsilon^{abc} W_M^b W_N^c$ is the field strength tensor for the $SU(2)_L$ electroweak gauge group, $B_{MN} = \partial_M B_N - \partial_N B_M$ is that of the $U(1)$ group, and all fields depend both on x and y . The covariant derivative is defined as $\mathcal{D}_M = \partial_M - i\tilde{g} W_M^a T^a - i\tilde{g}' B_M Y$, where \tilde{g} and \tilde{g}' are the five-dimensional gauge couplings for the $SU(2)_L$ and $U(1)$ groups. The five-dimensional Γ_M matrices are defined as $\Gamma^\mu = \gamma^\mu$, $\mu = 0, 1, 2, 3$ and $\Gamma^5 = i\gamma^5$.

In the case of a single extra dimension with coordinate $x_5 = y$ compactified on a circle of radius R , a field $F(x, y)$ would be periodic function of y , and hence can be written as

$$F(x, y) = \sum_{n=-\infty}^{+\infty} F_n(x) e^{iny/R}.$$

The Fourier expansions of the fields are

$$\begin{aligned} B_\mu(x, y) &= \frac{1}{\sqrt{2\pi R}} B_\mu^{(0)} + \frac{1}{\sqrt{\pi R}} \sum_{n=1}^{\infty} B_\mu^{(n)}(x) \cos\left(\frac{ny}{R}\right), \\ B_5(x, y) &= \frac{1}{\sqrt{\pi R}} \sum_{n=1}^{\infty} B_5^{(n)} \sin\left(\frac{ny}{R}\right), \\ \mathcal{Q}(x, y) &= \frac{1}{\sqrt{2\pi R}} \mathcal{Q}_L^{(0)} \\ &\quad + \frac{1}{\sqrt{\pi R}} \sum_{n=1}^{\infty} \left[\mathcal{Q}_L^{(n)} \cos\left(\frac{ny}{R}\right) + \mathcal{Q}_R^{(n)} \sin\left(\frac{ny}{R}\right) \right], \\ U(\mathcal{D})(x, y) &= \frac{1}{\sqrt{2\pi R}} U_R^{(0)} \\ &\quad + \frac{1}{\sqrt{\pi R}} \sum_{n=1}^{\infty} \left[U_R^{(n)} \cos\left(\frac{ny}{R}\right) + U_L^{(n)} \sin\left(\frac{ny}{R}\right) \right]. \end{aligned}$$

Under the parity transformation P_5 , $y \rightarrow -y$, fields having a corresponding field in the four-dimensional SM should be even, so that their zero-mode in the KK can be interpreted as the ordinary SM field, and all remaining new fields should be odd.

In the ACD model the KK parity is conserved. This conservation implies that there are no tree level diagrams with exchange of KK modes in low energy processes (at the scale $\mu \ll 1/R$), and a single KK excitation cannot be produced, i.e., these excitations appear only in pairs. Lastly, in the ACD model there are three additional physical scalar modes, $a_n^{(0)}$ and a_n^\pm . The zero-mode is either right-handed or left-handed.

The Lagrangian of the ACD model can be obtained by integrating over $x_5 = y$:

$$\mathcal{L}_4(x) = \int_0^{2\pi R} \mathcal{L}_5(x, y) dy.$$

Note that the zero-mode remains massless unless we apply the Higgs mechanism. All fields in the four-dimensional

Lagrangian receive the KK mass n/R on account of the derivative operator ∂_5 acting on them. The relevant Feynman rules are derived in [30] and for more details of the ACD model we refer the interested reader to [31, 32].

After this introduction, let us start to discuss the main problem, namely, double-lepton polarization asymmetries for $\Lambda_b \rightarrow \Lambda \ell^+ \ell^-$ decay.

At the quark level, $\Lambda_b \rightarrow \Lambda \ell^+ \ell^-$ decay is described by the $b \rightarrow s \ell^+ \ell^-$ transition. The effective Hamiltonian governing this transition in the SM with $\Delta B = -1$ and $\Delta S = 1$ is described in terms of a set of local operators:

$$\mathcal{H}_{\text{eff}} = \frac{4G_F}{\sqrt{2}} V_{tb} V_{ts}^* \sum_1^{10} C_i(\mu) \mathcal{O}_i(\mu), \quad (1)$$

where G_F is the Fermi constant, and V_{ij} are the elements of the Cabibbo–Kobayashi–Maskawa (CKM) matrix. The explicit forms of the operators, which are written in terms of quark and gluon fields, can be found in [34–36].

The Wilson coefficients in (1) have been computed at NNLO in the SM in [34–36]. At NLO these Wilson coefficients are calculated for the ACD model including the effects of KK modes, in [30, 31], which we have used in our calculations. It should be noted here that there does not appear any new operator in the ACD model, and therefore the effect of new particles leads to modification of the Wilson coefficients existing in the SM, if we neglect the contributions of the scalar fields, which are indeed very small.

At the $\mu = \mathcal{O}(m_W)$ level, only $C_2^{(0)}$, $C_7^{(0)}(m_W)$, $C_8^{(0)}(m_W)$, $C_9^{(0)}(m_W)$ and $C_{10}^{(0)}(m_W)$ are different from zero, and the remaining coefficients are all zero.

In the SM, at the quark level, $\Lambda_b \rightarrow \Lambda \ell^+ \ell^-$ decay is described by the following matrix element:

$$\begin{aligned} \mathcal{M} = & \frac{G_F \alpha}{4\sqrt{2}\pi} V_{tb} V_{ts}^* \left\{ -\frac{2m_b}{q^2} C_7^{\text{eff}} \bar{s} i \sigma_{\mu\nu} (1 + \gamma_5) q^\nu b \bar{\ell} \gamma^\mu \ell \right. \\ & \left. + C_9 \bar{s} \gamma_\mu (1 - \gamma_5) b \bar{\ell} \gamma^\mu \ell + C_{10} \bar{s} \gamma_\mu (1 - \gamma_5) b \bar{\ell} \gamma^\mu \gamma_5 \ell \right\}. \quad (2) \end{aligned}$$

As has already been noted, C_7^{eff} , C_9 and C_{10} are calculated in the SM in [34–36] (see also [37–40]).

Contributions coming from the UED model to these Wilson coefficients are calculated in [30, 31], which can be written as

$$\begin{aligned} C_7^{(0)}(\mu_W) &= -\frac{1}{2} D'(x_t, 1/R), \\ C_9^{(0)}(\mu) &= P_0^{\text{NDR}} + \frac{Y(x_t, 1/R)}{\sin^2 \theta_W} \\ &\quad - 4Z(x_t, 1/R) + P_E E(x_t, 1/R), \\ C_{10}^{(0)} &= -\frac{Y(x_t, 1/R)}{\sin^2 \theta_W}. \quad (3) \end{aligned}$$

Here $P_0^{\text{NDR}} = 2.60 \pm 0.25$, and the superscript (0) refers to the leading log approximation. Explicit expressions for the functions $D'(x_t, 1/R)$, $Y(x_t, 1/R)$ and $Z(x_t, 1/R)$ can be found in [30–32].

With these coefficients and the operators in (1) the inclusive $b \rightarrow s \ell^+ \ell^-$ transitions are studied in [30, 31].

The amplitude of exclusive $\Lambda_b \rightarrow \Lambda \ell^+ \ell^-$ decay is obtained by sandwiching the matrix element given in (2) between the initial and final baryon states $\langle \Lambda | \mathcal{M} | \Lambda_b \rangle$. It follows from (2) that the matrix elements

$$\begin{aligned} \langle \Lambda | \bar{s} \gamma_\mu (1 - \gamma_5) b | \Lambda_b \rangle, \\ \langle \Lambda | \bar{s} \sigma_{\mu\nu} (1 + \gamma_5) b | \Lambda_b \rangle \end{aligned} \quad (4)$$

are needed in order to calculate the $\Lambda_b \rightarrow \Lambda \ell^+ \ell^-$ decay amplitude.

These matrix elements, parametrized in terms of the form factors, are as follows [41–43]:

$$\begin{aligned} \langle \Lambda | \bar{s} \gamma_\mu b | \Lambda_b \rangle &= \bar{u}_\Lambda [f_1 \gamma_\mu + i f_2 \sigma_{\mu\nu} q^\nu + f_3 q_\mu] u_{\Lambda_b}, \quad (5) \\ \langle \Lambda | \bar{s} \gamma_\mu \gamma_5 b | \Lambda_b \rangle &= \bar{u}_\Lambda [g_1 \gamma_\mu \gamma_5 + i g_2 \sigma_{\mu\nu} \gamma_5 q^\nu + g_3 q_\mu \gamma_5] u_{\Lambda_b}, \quad (6) \end{aligned}$$

where $q = p_{\Lambda_b} - p_\Lambda$.

The form factors of the magnetic dipole operators are defined as

$$\begin{aligned} \langle \Lambda | \bar{s} i \sigma_{\mu\nu} q^\nu b | \Lambda_b \rangle &= \bar{u}_\Lambda [f_1^T \gamma_\mu + i f_2^T \sigma_{\mu\nu} q^\nu + f_3^T q_\mu] u_{\Lambda_b}, \\ \langle \Lambda | \bar{s} i \sigma_{\mu\nu} \gamma_5 q^\nu b | \Lambda_b \rangle &= \\ \bar{u}_\Lambda [g_1^T \gamma_\mu \gamma_5 + i g_2^T \sigma_{\mu\nu} \gamma_5 q^\nu + g_3^T q_\mu \gamma_5] u_{\Lambda_b}. \quad (7) \end{aligned}$$

Using the identity

$$\sigma_{\mu\nu} \gamma_5 = -\frac{i}{2} \epsilon_{\mu\nu\alpha\beta} \sigma^{\alpha\beta},$$

the following relations between the form factors are obtained:

$$\begin{aligned} f_1^T &= -\frac{q^2}{m_{\Lambda_b} - m_\Lambda} f_3^T, \\ g_1^T &= \frac{q^2}{m_{\Lambda_b} + m_\Lambda} g_3^T. \quad (8) \end{aligned}$$

Using these definitions of the form factors, for the matrix element of $\Lambda_b \rightarrow \Lambda \ell^+ \ell^-$ we get

$$\begin{aligned} \mathcal{M} = & \frac{G_F \alpha}{4\sqrt{2}\pi} V_{tb} V_{ts}^* \frac{1}{2} \\ & \times \left\{ \bar{\ell} \gamma_\mu (1 - \gamma_5) \ell \bar{u}_\Lambda [(A_1 - D_1) \gamma_\mu (1 + \gamma_5) \right. \\ & \quad + (B_1 - E_1) \gamma_\mu (1 - \gamma_5) \\ & \quad + i \sigma_{\mu\nu} q^\nu ((A_2 - D_2)(1 + \gamma_5) + (B_2 - E_2)(1 - \gamma_5)) \\ & \quad + q_\mu ((A_3 - D_3)(1 + \gamma_5) + (B_3 - E_3)(1 - \gamma_5))] \\ & \quad \times u_{\Lambda_b} + \bar{\ell} \gamma_\mu (1 + \gamma_5) \ell \bar{u}_\Lambda \\ & \quad \times [(A_1 + D_1) \gamma_\mu (1 + \gamma_5) + (B_1 + E_1) \gamma_\mu (1 - \gamma_5) \\ & \quad + i \sigma_{\mu\nu} q^\nu ((A_2 + D_2)(1 + \gamma_5) + (B_2 + E_2)(1 - \gamma_5)) \\ & \quad \left. + q_\mu ((A_3 + D_3)(1 + \gamma_5) + (B_3 + E_3)(1 - \gamma_5))] u_{\Lambda_b} \right\}, \quad (9) \end{aligned}$$

where

$$\begin{aligned}
 A_1 &= \frac{1}{q^2} (f_1^T - g_1^T) (-2m_s C_7) \\
 &\quad + \frac{1}{q^2} (f_1^T + g_1^T) (-2m_b C_7) + (f_1 - g_1) C_9^{\text{eff}}, \\
 A_2 &= A_1 (1 \rightarrow 2), \\
 A_3 &= A_1 (1 \rightarrow 3), \\
 B_1 &= A_1 (g_1 \rightarrow -g_1; g_1^T \rightarrow -g_1^T), \\
 B_2 &= B_1 (1 \rightarrow 2), \\
 B_3 &= B_1 (1 \rightarrow 3), \\
 D_1 &= C_{10} (f_1 - g_1), \\
 D_2 &= D_1 (1 \rightarrow 2), \\
 D_3 &= D_1 (1 \rightarrow 3), \\
 E_1 &= D_1 (g_1 \rightarrow -g_1), \\
 E_2 &= E_1 (1 \rightarrow 2), \\
 E_3 &= E_1 (1 \rightarrow 3).
 \end{aligned} \tag{10}$$

From these expressions it follows that $\Lambda_b \rightarrow \Lambda \ell^+ \ell^-$ decay is described in terms of many form factors. It is shown in [6] (see also [44]) that heavy quark effective theory (HQET) reduces the number of independent form factors to two (F_1 and F_2) irrespective of the Dirac structure of the corresponding operators, i.e.,

$$\langle \Lambda(p_\Lambda) | \bar{s} \Gamma b | \Lambda(p_{\Lambda_b}) \rangle = \bar{u}_\Lambda [F_1(q^2) + \not{v} F_2(q^2)] \Gamma u_{\Lambda_b}, \tag{11}$$

where Γ is an arbitrary Dirac structure and $v^\mu = p_{\Lambda_b}^\mu / m_{\Lambda_b}$ is the four-velocity of Λ_b . Comparing the general form of the form factors given in (5)–(7) with the ones given in (11), one can easily obtain the following relations [41, 43]:

$$\begin{aligned}
 g_1 &= f_1 = f_2^T = g_2^T = F_1 + \sqrt{\hat{r}_\Lambda} F_2, \\
 g_2 &= f_2 = g_3 = f_3 = \frac{F_2}{m_{\Lambda_b}}, \\
 g_1^T &= f_1^T = \frac{F_2}{m_{\Lambda_b}} q^2, \\
 g_3^T &= \frac{F_2}{m_{\Lambda_b}} (m_{\Lambda_b} + m_\Lambda), \\
 f_3^T &= -\frac{F_2}{m_{\Lambda_b}} (m_{\Lambda_b} - m_\Lambda),
 \end{aligned} \tag{12}$$

where $\hat{r}_\Lambda = m_\Lambda^2 / m_{\Lambda_b}^2$.

As we have already noted, our purpose is the calculation of double-lepton polarizations in the UED model.

For calculation of the double-lepton polarization asymmetries, the following orthogonal unit vectors $s_i^{\pm\mu}$ in the rest frame of ℓ^\pm ($i = L, T$ or N stand for longitudinal, transversal or normal polarizations, respectively) are chosen as

$$s_L^{-\mu} = (0, \mathbf{e}_L^-) = \left(0, \frac{\mathbf{p}_-}{|\mathbf{p}_-|}\right),$$

$$\begin{aligned}
 s_N^{-\mu} &= (0, \mathbf{e}_N^-) = \left(0, \frac{\mathbf{p}_\Lambda \times \mathbf{p}_-}{|\mathbf{p}_\Lambda \times \mathbf{p}_-|}\right), \\
 s_T^{-\mu} &= (0, \mathbf{e}_T^-) = (0, \mathbf{e}_N^- \times \mathbf{e}_L^-), \\
 s_L^{+\mu} &= (0, \mathbf{e}_L^+) = \left(0, \frac{\mathbf{p}_+}{|\mathbf{p}_+|}\right), \\
 s_N^{+\mu} &= (0, \mathbf{e}_N^+) = \left(0, \frac{\mathbf{p}_\Lambda \times \mathbf{p}_+}{|\mathbf{p}_\Lambda \times \mathbf{p}_+|}\right), \\
 s_T^{+\mu} &= (0, \mathbf{e}_T^+) = (0, \mathbf{e}_N^+ \times \mathbf{e}_L^+),
 \end{aligned} \tag{13}$$

where \mathbf{p}_\mp and \mathbf{p}_Λ are the three-momenta of the leptons ℓ^\mp and of the Λ baryon in the center of mass frame (CM) of the $\ell^- \ell^+$ system, respectively. Transformation of the unit vectors from the rest frame of the leptons to the CM frame of the leptons can be done by a Lorentz boost. Boosting of the longitudinal unit vectors $s_L^{\pm\mu}$ yields

$$(s_L^{\mp\mu})_{\text{CM}} = \left(\frac{|\mathbf{p}_\mp|}{m_\ell}, \frac{E_\ell \mathbf{p}_\mp}{m_\ell |\mathbf{p}_\mp|}\right), \tag{14}$$

where $\mathbf{p}_+ = -\mathbf{p}_-$, E_ℓ and m_ℓ are the energy and mass of the leptons in the CM frame, respectively. The remaining two unit vectors, $s_N^{\pm\mu}$ and $s_T^{\pm\mu}$, are unchanged under a Lorentz boost.

The double-polarization asymmetries are defined in the following way [24]:

$$\begin{aligned}
 P_{ij}(q^2) &= \left[\left(\frac{d\Gamma(\mathbf{s}_i^-, \mathbf{s}_j^+)}{dq^2} - \frac{d\Gamma(-\mathbf{s}_i^-, \mathbf{s}_j^+)}{dq^2} \right) \right. \\
 &\quad \left. - \left(\frac{d\Gamma(\mathbf{s}_i^-, -\mathbf{s}_j^+)}{dq^2} - \frac{d\Gamma(-\mathbf{s}_i^-, -\mathbf{s}_j^+)}{dq^2} \right) \right] \\
 &\quad / \left[\left(\frac{d\Gamma(\mathbf{s}_i^-, \mathbf{s}_j^+)}{dq^2} + \frac{d\Gamma(-\mathbf{s}_i^-, \mathbf{s}_j^+)}{dq^2} \right) \right. \\
 &\quad \left. + \left(\frac{d\Gamma(\mathbf{s}_i^-, -\mathbf{s}_j^+)}{dq^2} + \frac{d\Gamma(-\mathbf{s}_i^-, -\mathbf{s}_j^+)}{dq^2} \right) \right],
 \end{aligned} \tag{15}$$

where the first subindex i represents the lepton and the second one the antilepton. Using this definition of P_{ij} , nine double-lepton polarization asymmetries are calculated. Their expressions are

$$\begin{aligned}
 P_{LL} &= \frac{16m_{\Lambda_b}^4}{3\Delta} \text{Re} \left\{ -6m_{\Lambda_b} \sqrt{\hat{r}_\Lambda} (1 - \hat{r}_\Lambda + \hat{s}) \right. \\
 &\quad \times \left[\hat{s} (1 + v^2) (A_1 A_2^* + B_1 B_2^*) \right. \\
 &\quad \left. \left. - 4\hat{m}_\ell^2 (D_1 D_3^* + E_1 E_3^*) \right] \right. \\
 &\quad + 6m_{\Lambda_b} (1 - \hat{r}_\Lambda - \hat{s}) \left[\hat{s} (1 + v^2) (A_1 B_2^* + A_2 B_1^*) \right. \\
 &\quad \left. \left. + 4\hat{m}_\ell^2 (D_1 E_3^* + D_3 E_1^*) \right] \right. \\
 &\quad + 12\sqrt{\hat{r}_\Lambda} \hat{s} (1 + v^2) \left(A_1 B_1^* + D_1 E_1^* + m_{\Lambda_b}^2 \hat{s} A_2 B_2^* \right) \\
 &\quad \left. + 12m_{\Lambda_b}^2 \hat{m}_\ell^2 \hat{s} (1 + \hat{r}_\Lambda - \hat{s}) \left(|D_3|^2 + |E_3^*|^2 \right) \right\}
 \end{aligned}$$

$$\begin{aligned}
 & - (1+v^2) \left[1 + \hat{r}_\Lambda^2 - \hat{r}_\Lambda (2 - \hat{s}) + \hat{s}(1 - 2\hat{s}) \right] \\
 & \times \left(|A_1|^2 + |B_1|^2 \right) \\
 & - \left[(5v^2 - 3)(1 - \hat{r}_\Lambda)^2 + 4\hat{m}_\ell^2(1 + \hat{r}_\Lambda) \right. \\
 & \left. + 2\hat{s}(1 + 8\hat{m}_\ell^2 + \hat{r}_\Lambda) - 4\hat{s}^2 \right] \\
 & \times \left(|D_1|^2 + |E_1|^2 \right) \\
 & - m_{\Lambda_b}^2 (1+v^2) \hat{s} \left[2 + 2\hat{r}_\Lambda^2 - \hat{s}(1 + \hat{s}) - \hat{r}_\Lambda(4 + \hat{s}) \right] \\
 & \times \left(|A_2|^2 + |B_2|^2 \right) \\
 & - 2m_{\Lambda_b}^2 \hat{s} v^2 \left[2(1 + \hat{r}_\Lambda^2) - \hat{s}(1 + \hat{s}) - \hat{r}_\Lambda(4 + \hat{s}) \right] \\
 & \times \left(|D_2|^2 + |E_2|^2 \right) \\
 & + 12m_{\Lambda_b} \hat{s} (1 - \hat{r}_\Lambda - \hat{s}) v^2 (D_1 E_2^* + D_2 E_1^*) \\
 & - 12m_{\Lambda_b} \sqrt{\hat{r}_\Lambda} \hat{s} (1 - \hat{r}_\Lambda + \hat{s}) v^2 (D_1 D_2^* + E_1 E_2^*) \\
 & \left. + 24m_{\Lambda_b}^2 \sqrt{\hat{r}_\Lambda} \hat{s} (\hat{s} v^2 D_2 E_2^* + 2\hat{m}_\ell^2 D_3 E_3^*) \right\}, \quad (16)
 \end{aligned}$$

$$\begin{aligned}
 P_{LN} = & \frac{16\pi m_{\Lambda_b}^4 \hat{m}_\ell \sqrt{\lambda}}{\Delta \sqrt{\hat{s}}} \text{Im} \left\{ (1 - \hat{r}_\Lambda) (A_1^* D_1 + B_1^* E_1) \right. \\
 & + m_{\Lambda_b} \hat{s} (A_1^* E_3 - A_2^* E_1 + B_1^* D_3 - B_2^* D_1) \\
 & + m_{\Lambda_b} \sqrt{\hat{r}_\Lambda} \hat{s} (A_1^* D_3 + A_2^* D_1 + B_1^* E_3 + B_2^* E_1) \\
 & \left. - m_{\Lambda_b}^2 \hat{s}^2 (B_2^* E_3 + A_2^* D_3) \right\}, \quad (17)
 \end{aligned}$$

$$\begin{aligned}
 P_{NL} = & -\frac{16\pi m_{\Lambda_b}^4 \hat{m}_\ell \sqrt{\lambda}}{\Delta \sqrt{\hat{s}}} \text{Im} \left\{ (1 - \hat{r}_\Lambda) (A_1^* D_1 + B_1^* E_1) \right. \\
 & + m_{\Lambda_b} \hat{s} (A_1^* E_3 - A_2^* E_1 + B_1^* D_3 - B_2^* D_1) \\
 & - m_{\Lambda_b} \sqrt{\hat{r}_\Lambda} \hat{s} (A_1^* D_3 + A_2^* D_1 + B_1^* E_3 + B_2^* E_1) \\
 & \left. - m_{\Lambda_b}^2 \hat{s}^2 (B_2^* E_3 + A_2^* D_3) \right\}, \quad (18)
 \end{aligned}$$

$$\begin{aligned}
 P_{LT} = & \frac{16\pi m_{\Lambda_b}^4 \hat{m}_\ell \sqrt{\lambda} v}{\Delta \sqrt{\hat{s}}} \text{Re} \left\{ (1 - \hat{r}_\Lambda) \left(|D_1|^2 + |E_1|^2 \right) \right. \\
 & - \hat{s} (A_1 D_1^* - B_1 E_1^*) \\
 & - m_{\Lambda_b} \hat{s} [B_1 D_2^* + (A_2 + D_2 - D_3) E_1^* - A_1 E_2^* \\
 & \left. - (B_2 - E_2 + E_3) D_1^*] \right. \\
 & + m_{\Lambda_b} \sqrt{\hat{r}_\Lambda} \hat{s} [A_1 D_2^* + (A_2 + D_2 + D_3) D_1^* \\
 & \left. - B_1 E_2^* - (B_2 - E_2 - E_3) E_1^*] \right. \\
 & + m_{\Lambda_b}^2 \hat{s} (1 - \hat{r}_\Lambda) (A_2 D_2^* - B_2 E_2^*) \\
 & \left. - m_{\Lambda_b}^2 \hat{s}^2 (D_2 D_3^* + E_2 E_3^*) \right\}, \quad (19)
 \end{aligned}$$

$$\begin{aligned}
 P_{TL} = & \frac{16\pi m_{\Lambda_b}^4 \hat{m}_\ell \sqrt{\lambda} v}{\Delta \sqrt{\hat{s}}} \text{Re} \left\{ (1 - \hat{r}_\Lambda) \left(|D_1|^2 + |E_1|^2 \right) \right. \\
 & + \hat{s} (A_1 D_1^* - B_1 E_1^*) \\
 & + m_{\Lambda_b} \hat{s} [B_1 D_2^* + (A_2 - D_2 + D_3) E_1^* - A_1 E_2^* \\
 & \left. - (B_2 + E_2 - E_3) D_1^*] \right. \\
 & - m_{\Lambda_b} \sqrt{\hat{r}_\Lambda} \hat{s} [A_1 D_2^* + (A_2 - D_2 - D_3) D_1^* - B_1 E_2^* \\
 & \left. - (B_2 + E_2 + E_3) E_1^*] \right\}
 \end{aligned}$$

$$\begin{aligned}
 & - m_{\Lambda_b}^2 \hat{s} (1 - \hat{r}_\Lambda) (A_2 D_2^* - B_2 E_2^*) \\
 & - m_{\Lambda_b}^2 \hat{s}^2 (D_2 D_3^* + E_2 E_3^*) \left. \right\}, \quad (20)
 \end{aligned}$$

$$\begin{aligned}
 P_{NT} = & \frac{64m_{\Lambda_b}^4 \lambda v}{3\Delta} \text{Im} \left\{ (A_1 D_1^* + B_1 E_1^*) + m_{\Lambda_b}^2 \hat{s} (A_2^* D_2 + B_2^* E_2) \right\}, \quad (21)
 \end{aligned}$$

$$\begin{aligned}
 P_{TN} = & -\frac{64m_{\Lambda_b}^4 \lambda v}{3\Delta} \text{Im} \left\{ (A_1 D_1^* + B_1 E_1^*) + m_{\Lambda_b}^2 \hat{s} (A_2^* D_2 + B_2^* E_2) \right\}, \quad (22)
 \end{aligned}$$

$$\begin{aligned}
 P_{NN} = & \frac{32m_{\Lambda_b}^4}{3\hat{s}\Delta} \text{Re} \left\{ 24\hat{m}_\ell^2 \sqrt{\hat{r}_\Lambda} \hat{s} (A_1 B_1^* + D_1 E_1^*) \right. \\
 & - 12m_{\Lambda_b} \hat{m}_\ell^2 \sqrt{\hat{r}_\Lambda} \hat{s} (1 - \hat{r}_\Lambda + \hat{s}) (A_1 A_2^* + B_1 B_2^*) \\
 & + 6m_{\Lambda_b} \hat{m}_\ell^2 \hat{s} \left[m_{\Lambda_b} \hat{s} (1 + \hat{r}_\Lambda - \hat{s}) \left(|D_3|^2 + |E_3|^2 \right) \right. \\
 & \left. + 2\sqrt{\hat{r}_\Lambda} (1 - \hat{r}_\Lambda + \hat{s}) (D_1 D_3^* + E_1 E_3^*) \right] \\
 & + 12m_{\Lambda_b} \hat{m}_\ell^2 \hat{s} (1 - \hat{r}_\Lambda - \hat{s}) \\
 & \times (A_1 B_2^* + A_2 B_1^* + D_1 E_3^* + D_3 E_1^*) \\
 & - [\lambda \hat{s} + 2\hat{m}_\ell^2 (1 + \hat{r}_\Lambda^2 - 2\hat{r}_\Lambda + \hat{r}_\Lambda \hat{s} + \hat{s} - 2\hat{s}^2)] \\
 & \times \left(|A_1|^2 + |B_1|^2 - |D_1|^2 - |E_1|^2 \right) \\
 & + 24m_{\Lambda_b}^2 \hat{m}_\ell^2 \sqrt{\hat{r}_\Lambda} \hat{s}^2 (A_2 B_2^* + D_3 E_3^*) - m_{\Lambda_b}^2 \lambda \hat{s}^2 v^2 \\
 & \times \left(|D_2|^2 + |E_2|^2 \right) \\
 & + m_{\Lambda_b}^2 \hat{s} \\
 & \times \left\{ \lambda \hat{s} - 2\hat{m}_\ell^2 [2(1 + \hat{r}_\Lambda^2) - \hat{s}(1 + \hat{s}) - \hat{r}_\Lambda(4 + \hat{s})] \right\} \\
 & \left. \times \left(|A_2|^2 + |B_2|^2 \right) \right\}, \quad (23)
 \end{aligned}$$

$$\begin{aligned}
 P_{TT} = & \frac{32m_{\Lambda_b}^4}{3\hat{s}\Delta} \text{Re} \left\{ -24\hat{m}_\ell^2 \sqrt{\hat{r}_\Lambda} \hat{s} (A_1 B_1^* + D_1 E_1^*) \right. \\
 & - 12m_{\Lambda_b} \hat{m}_\ell^2 \sqrt{\hat{r}_\Lambda} \hat{s} (1 - \hat{r}_\Lambda + \hat{s}) (D_1 D_3^* + E_1 E_3^*) \\
 & - 24m_{\Lambda_b}^2 \hat{m}_\ell^2 \sqrt{\hat{r}_\Lambda} \hat{s}^2 (A_2 B_2^* + D_3 E_3^*) \\
 & - 6m_{\Lambda_b} \hat{m}_\ell^2 \hat{s} \left[m_{\Lambda_b} \hat{s} (1 + \hat{r}_\Lambda - \hat{s}) \left(|D_3|^2 + |E_3|^2 \right) \right. \\
 & \left. - 2\sqrt{\hat{r}_\Lambda} (1 - \hat{r}_\Lambda + \hat{s}) (A_1 A_2^* + B_1 B_2^*) \right] \\
 & - 12m_{\Lambda_b} \hat{m}_\ell^2 \hat{s} (1 - \hat{r}_\Lambda - \hat{s}) \\
 & \times (A_1 B_2^* + A_2 B_1^* + D_1 E_3^* + D_3 E_1^*) \\
 & - [\lambda \hat{s} - 2\hat{m}_\ell^2 (1 + \hat{r}_\Lambda^2 - 2\hat{r}_\Lambda + \hat{r}_\Lambda \hat{s} + \hat{s} - 2\hat{s}^2)] \\
 & \times \left(|A_1|^2 + |B_1|^2 \right) \\
 & + m_{\Lambda_b}^2 \hat{s} \left\{ \lambda \hat{s} + \hat{m}_\ell^2 [4(1 - \hat{r}_\Lambda)^2 - 2\hat{s}(1 + \hat{r}_\Lambda) - 2\hat{s}^2] \right\} \\
 & \times \left(|A_2|^2 + |B_2|^2 \right) \\
 & + \left\{ \lambda \hat{s} - 2\hat{m}_\ell^2 [5(1 - \hat{r}_\Lambda)^2 - 7\hat{s}(1 + \hat{r}_\Lambda) + 2\hat{s}^2] \right\} \\
 & \times \left(|D_1|^2 + |E_1|^2 \right) \\
 & \left. - m_{\Lambda_b}^2 \lambda \hat{s}^2 v^2 \left(|D_2|^2 + |E_2|^2 \right) \right\}. \quad (24)
 \end{aligned}$$

The explicit expression for Δ appearing in P_{ij} can be found in [43].

3 Numerical results

In this section we present our numerical results for the double-polarization asymmetries. The values of the input parameters we need in performing the numerical calculations are $|V_{tb}V_{ts}^*| = 0.0385$, $m_\tau = 1.77$ GeV, $m_\mu = 0.106$ GeV, $m_b = 4.8$ GeV [45], $m_t = 172.7$ GeV [46] and $\tau_{B_0} = (1.527 \pm 0.008)$ ps.

The $\Lambda_b \rightarrow \Lambda$ transition form factors are the main input parameters in performing the numerical analysis, which are embedded into the expressions of the double-lepton polarization asymmetries. The analysis of all form factors responsible for the $\Lambda_b \rightarrow \Lambda$ transition has not been accomplished so far. Therefore, for the form factors we will use the results coming from QCD sum rules in cooperation with HQET [42, 47], which reduce the number of independent form factors to two, and their q^2 dependence are given in terms of a three-parameter fit as follows:

$$F_i(\hat{s}) = \frac{F(0)}{1 - a_F \hat{s} + b_F \hat{s}^2}.$$

The values of the parameters $F(0)$, a_F and b_F are given in Table 1.

In numerical calculations we take into account the errors in the form factors. The errors in $F_1(0)$ and $F_2(0)$ are estimated to be ± 0.03 for each of the form factors in the framework of the QCD sum rule method [47].

The analysis of the double-lepton polarization asymmetries leads to the following results.

- P_{LL} in UED for $\Lambda_b \rightarrow \Lambda \mu^+ \mu^-$ decay practically coincides with the SM result, for all values of q^2 .
- For the $\Lambda_b \rightarrow \Lambda \tau^+ \tau^-$ case the difference between the predictions of SM and UED is substantial at $q^2 = 12$ GeV², i.e., $(P_{LL})_{UED} = 1.5 \times (P_{LL})_{SM}$ at $1/R = 250$ GeV; with increasing q^2 the difference between the two models decreases, but they never coincide (see Fig. 1). From this figure we see that when the errors in the form factors are taken into account, the results do not practically depart from the results obtained using their central values.
- For the $\Lambda_b \rightarrow \Lambda \mu^+ \mu^-$ decay, starting from $q^2 = 1$ GeV² up to the end of the spectrum, the value of P_{TT} in the SM is larger compared to that of the one predicted by the UED model. Especially, up to $q^2 = 10$ GeV², $(P_{TT})_{SM} = 2 \times (P_{TT})_{UED}$ (see Fig. 2).

Table 1. Form factors for $\Lambda_b \rightarrow \Lambda \ell^+ \ell^-$ decay in a three parameter fit

	$F(0)$	a_F	b_F
F_1	0.462	-0.0182	-0.000176
F_2	-0.077	-0.0685	0.00146

Therefore, measurement of the values of P_{LL} for $\Lambda_b \rightarrow \Lambda \tau^+ \tau^-$ decay and P_{TT} for $\Lambda_b \rightarrow \Lambda \mu^+ \mu^-$ decay can give quite important information on the presence of new physics beyond the SM.

- For $\Lambda_b \rightarrow \Lambda \tau^+ \tau^-$ decay, the difference between the predictions of the SM and UED is maximally about 60%, i.e., in terms of moduli, $|(P_{LT})_{UED}| > |(P_{LT})_{SM}|$, which can also be very useful for establishing new physics (see Fig. 4). The upper (lower) line in this figure corresponds to the cases when the error is added (subtracted) to the central values of the form factors. We observe that the departure of the results constitutes maximally 20% from the ones obtained using the central values of the form factors, and they are essentially distinguishable near the end of the invariant mass distribution.
- The maximum value of the difference between the SM and UED models concerning P_{TN} , P_{NT} , P_{LN} , P_{NL} and P_{TL} (excluding the $q^2 = 1$ GeV² region for the $\Lambda_b \rightarrow \Lambda \mu^+ \mu^-$ channel) for both decay channels is about 10%. Note that at $q^2 = 1$ GeV², $(P_{LT})_{UED} = (P_{TL})_{UED} \simeq 2 \times (P_{LT})_{SM} = 2 \times (P_{TL})_{SM}$, for $\Lambda_b \rightarrow \Lambda \mu^+ \mu^-$ decay.

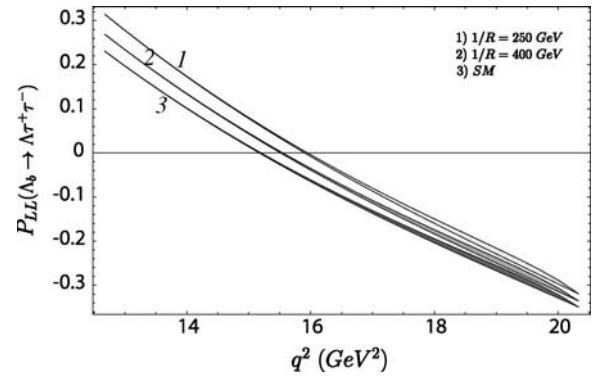


Fig. 1. The dependence of P_{LL} on q^2 for the $\Lambda_b \rightarrow \Lambda \tau^+ \tau^-$ decay at fixed values of the compactification parameter $1/R$. Here and in all following figures the *upper (lower) line* corresponds to the cases when the error is added (subtracted) to the central values of the form factors. For completeness, here and in all following figures, SM results are also given

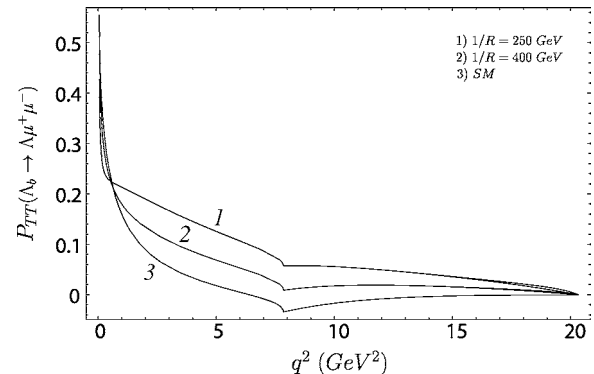


Fig. 2. The dependence of P_{TT} on q^2 for the $\Lambda_b \rightarrow \Lambda \mu^+ \mu^-$ decay at fixed values of the compactification parameter $1/R$

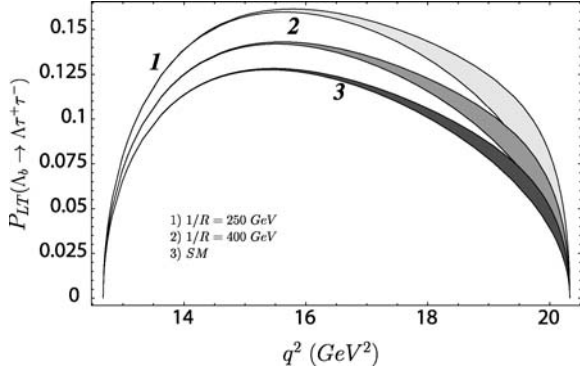


Fig. 3. The same as in Fig. 1, but for P_{LT}

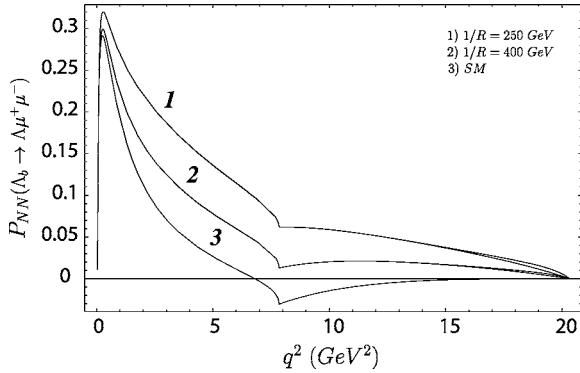


Fig. 4. The same as in Fig. 2, but for P_{NN}

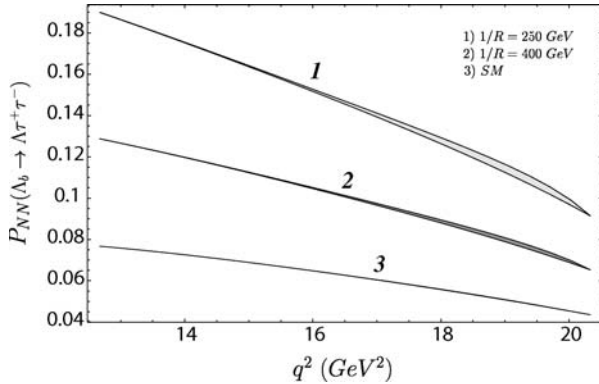


Fig. 5. The same as in Fig. 1, but for P_{NN}

- When $2 \text{ GeV}^2 \leq q^2 \leq 10 \text{ GeV}^2$, the prediction of the UED model for P_{NN} is maximally two times larger than the SM prediction for the $\Lambda_b \rightarrow \Lambda \mu^+ \mu^-$ decay (see Fig. 3).
- As far as P_{NN} for the $\Lambda_b \rightarrow \Lambda \tau^+ \tau^-$ decay is concerned, the situation is more promising. When the momentum transfer square q^2 varies in the region $14 \text{ GeV}^2 \leq q^2 \leq 18 \text{ GeV}^2$, the difference between the results of the two models on P_{NN} is quite large, about 2.5 times; i.e., $(P_{NN})_{UED} \simeq 2.5 \times (P_{NN})_{SM}$, and it may be measurable in the experiments (see Fig. 5).

From the above-presented discussion we conclude that measurement of various double-lepton polarization asym-

metries can be very useful for establishing new physics predicted by the UED model. Here we should note that single-lepton polarization is not a suitable tool for discrimination of the UED model and SM [34–36].

In conclusion, we study the double-lepton polarization asymmetries in the UED model. We find that various double-lepton polarization asymmetries are very sensitive to the UED model, and the results are substantially different from the ones obtained in the SM, and hence can serve as a promising tool for establishing new physics beyond the SM.

Acknowledgements. One of the authors (T.M.A) is grateful to TÜBİTAK for partial support of this work under the project 105T131.

References

1. T.M. Aliev, M. Savcı, JHEP **05**, 1 (2006)
2. BELLE Collaboration, K. Abe et al., hep-ex/0410006
3. BELLE Collaboration, M. Iwasaki et al., Phys. Rev. D **72**, 092005 (2005)
4. BaBar Collaboration, B. Aubert et al., hep-ex/0507005
5. BaBar Collaboration, B. Aubert et al., Phys. Rev. Lett. **93**, 081802 (2004)
6. T. Mannel, S. Recksiegel, J. Phys. G **24**, 979 (1998)
7. P. Bialas, J.G. Körner, M. Krämer, K. Zalewski, Z. Phys. C **57**, 115 (1993)
8. F. Hussain, J.G. Körner, R. Migneron, Phys. Lett. B **248**, 406 (1990)
9. F. Hussain, J.G. Körner, R. Migneron, Z. Phys. C **252**, 723(E) (1990)
10. J.G. Körner, M. Krämer, Phys. Lett. B **275**, 495 (1992)
11. T. Mannel, G.A. Schuler, Phys. Rev. D **279**, 194 (1992)
12. M. Gronau, S. Wakaizumi, Phys. Rev. D **47**, 1262 (1993)
13. M. Tanaka, Phys. Rev. D **47**, 4969 (1993)
14. M. Gronau, T. Hasuike, T. Hattori, Z. Hioki, T. Hayashi, S. Wakaizumi, J. Phys. G **19**, 1987 (1993)
15. Z. Hioki, Z. Phys. C **59**, 555 (1993)
16. B. König, J.G. Körner, M. Krämer, Phys. Rev. D **49**, 2363 (1994)
17. M. Gremm, G. Köpp, L.M. Sehgal, Phys. Rev. D **52**, 1588 (1995)
18. C.S. Huang, H.G. Yan, Phys. Rev. D **56**, 5981 (1997)
19. S. Balk, J.G. Körner, D. Pirjol, Eur. Phys. J. C **1**, 221 (1998)
20. J.G. Körner, D. Pirjol, Phys. Lett. B **334**, 399 (1994)
21. J.G. Körner, D. Pirjol, Phys. Rev. D **60**, 014021 (1999)
22. J.G. Körner, M. Krämer, D. Pirjol, Prog. Part. Nucl. Phys. **33**, 787 (1994)
23. Z. Zhao et al., Report of Snowmass 2001 working group E2: Electron Positron Colliders from the ϕ to the Z , in Proc. of the APS/DPF/DPB Summer Study on the Future of Particle Physics (Snowmass 2001) ed. by R. Davidson, C. Quigg, hep-ex/0201047
24. W. Bensalem, D. London, N. Sinha, R. Sinha, Phys. Rev. D **67**, 034007 (2003)
25. T. Appelquist, H.C. Cheng, B.A. Dobrescu, Phys. Rev. D **64**, 035002 (2001)

26. I. Antoniadis, Phys. Lett. B **246**, 317 (1990)
27. K. Agashe, N.G. Deshpande, G.H. Wu, Phys. Lett. B **511**, 85 (2001)
28. T. Appelquist, B.A. Dobrescu, Phys. Lett. B **516**, 85 (2001)
29. J.F. Oliver, J. Papavissiliou, A. Santamaria, Phys. Rev. D **67**, 056002 (2002)
30. A.J. Buras, M. Sprangler, A. Weiler, Nucl. Phys. B **660**, 225 (2003)
31. A.J. Buras, A. Poschenrieder, M. Spranger, Nucl. Phys. B **678**, 455 (2004)
32. P. Colangelo, F. De Fazio, R. Ferrandes, T.N. Pham, hep-ph/0604029
33. T.M. Aliev, M. Savcı, Eur. Phys. J. C **50**, 91 (2007)
34. C. Bobeth, M. Misiak, J. Urban, Nucl. Phys. B **574**, 291 (2001)
35. A. Ghinculov, T. Hurth, G. Isidori, Y.P. Yao, Nucl. Phys. B **685**, 351 (2004)
36. C. Bobeth, P. Cambino, M. Gorbahn, U. Haisch, JHEP **0404**, 071 (2004)
37. A. Buras, M. Misiak, M. Münz, S. Pokorski, Nucl. Phys. B **424**, 374 (1994)
38. M. Misiak, Nucl. Phys. B **393**, 23 (1993)
39. M. Misiak, Nucl. Phys. B **439**, 161 (1995)
40. B. Buras, M. Münz, Phys. Rev. D **52**, 186 (1995)
41. T.M. Aliev, A. Özpıneci, M. Savcı, Nucl. Phys. B **649**, 1681 (2003)
42. C.H. Chen, C.Q. Geng, Phys. Rev. D **64**, 074001 (2001)
43. T.M. Aliev, A. Özpıneci, M. Savcı, Phys. Rev. D **67**, 035007 (2003)
44. T. Mannel, W. Roberts, Z. Ryzak, Nucl. Phys. B **355**, 38 (1991)
45. Particle Data Group, W.M. Yao et al., J. Phys. G **33**, 1 (2006)
46. CDF Collaboration, hep-ex/0507091
47. C.S. Huang, H.G. Yan, Phys. Rev. D **59**, 114022 (1999)